HHS Public Access

Author manuscript

Immunity. Author manuscript; available in PMC 2016 November 17.

Published in final edited form as:

Immunity. 2015 November 17; 43(5): 870–883. doi:10.1016/j.immuni.2015.10.007.

The PIAS-like coactivator Zmiz1 is a direct and selective cofactor of Notch1 in T-cell development and leukemia

Nancy Pinnell[1,*], **Ran Yan**[2,*], **Hyo Je Cho**[3], **Theresa Keeley**[4], **Marcelo J. Murai**[3], **Yiran Liu**[2], **Amparo Serna Alarcon**[2], **Jason Qin**[2], **Qing Wang**[2], **Rork Kuick**[5], **Kojo S.J. Elenitoba-Johnson**[6], **Ivan Maillard**[2,7], **Linda C. Samuelson**[2,4], **Tomasz Cierpicki**[3], and **Mark Y. Chiang**[2]

[1]Cancer Biology Graduate Program, University of Michigan, Ann Arbor, MI, 48109, USA

[2]Department of Internal Medicine, University of Michigan, Ann Arbor, MI, 48109, USA

[3]Department of Pathology, University of Michigan, Ann Arbor, MI, 48109, USA

[4]Department of Molecular and Integrative Physiology, University of Michigan, Ann Arbor, MI, 48109, USA

[5]Department of Biostatistics, University of Michigan, Ann Arbor, MI, 48109, USA

[6]Department of Pathology, University of Pennsylvania, Philadelphia, PA, 19104, USA

[7]Life Sciences Institute, University of Michigan, Ann Arbor, MI, 48109, USA

Summary

Pan-NOTCH inhibitors are poorly tolerated in clinical trials because NOTCH signals are crucial for intestinal homeostasis. These inhibitors may also promote cancer as NOTCH can act as a tumor suppressor. We previously reported that the PIAS-like coactivator ZMIZ1 is frequently co-expressed with activated NOTCH1 in T-cell acute lymphoblastic leukemia (T-ALL). Here, we show that similar to Notch1, Zmiz1 was important for T-cell development and controlled the expression of certain Notch target genes, such as *Myc*. However, unlike Notch, Zmiz1 had no major role in intestinal homeostasis or myeloid suppression. Deletion of Zmiz1 impaired the initiation and maintenance of Notch-induced T-ALL. Zmiz1 directly interacted with Notch1 via a tetratricopeptide repeat domain at a special class of Notch-regulatory sites. In contrast to the Notch cofactor Maml, which is nonselective, Zmiz1 was selective. Thus, targeting the NOTCH1-ZMIZ1 interaction may combat leukemic growth while avoiding the intolerable toxicities of NOTCH inhibitors.

Graphical Abstract

Contact: Mark Y. Chiang, markchia@umich.edu.
*These authors contributed equally

Author Contributions

M.C., I.M., N.P., R.Y., K.E., L.S., and T.C. designed experiments and wrote the paper. R.K. wrote the paper and provided statistics. N.P., R.Y., Y.L., J.Q., M.C., T.K., H.C, M.M, and A.A. conducted experiments.

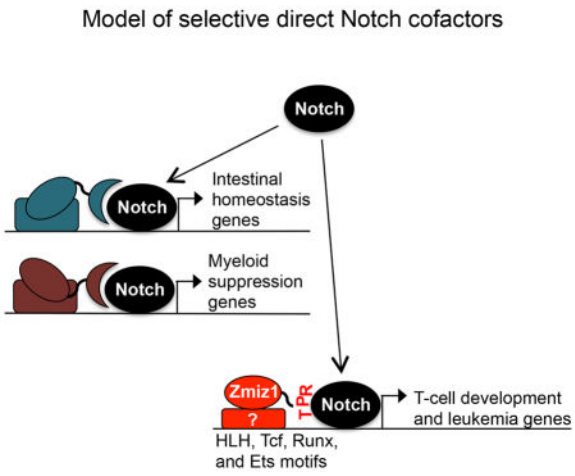

Introduction

The NOTCH pathway was first widely implicated in the pathogenesis of a human cancer with the identification of activating *NOTCH1* mutations in approximately 60% of cases of pediatric T-cell acute lymphoblastic leukemia/lymphoma (T-ALL)(Weng et al., 2004). Since then, NOTCH has been implicated as an oncogene in diverse cancers. These discoveries have raised hopes for NOTCH-targeted drugs to be broadly effective as anti-cancer agents. This is particularly important for relapsed T-ALL, which occurs in ~25% of cases and carries a dismal prognosis. Current treatments of T-ALL rely on cytotoxic drugs that have detrimental side effects. However, effective treatment of cancer with NOTCH inhibitors has been elusive. The most widely studied pan-NOTCH inhibitors are gamma-secretase inhibitors (GSIs), which block the cleavage of the NOTCH receptors (NOTCH1-4). NOTCH is initially activated by ligand (in cancer and normal cells) or by a mutation in some cancers such as T-ALL. Gamma-secretase then cleaves NOTCH, which releases the Intracellular domain of NOTCH(ICN). ICN translocates to the nucleus where it directly binds MAML cofactors and the DNA binding factor RBPJ to activate transcription of NOTCH target genes. Hence, GSIs deprive both cancer and normal cells of all ICN-driven signals. Clinical trials have shown that GSIs must be used intermittently, such as weekly dosing, because of intolerable adverse effects, particularly diarrhea(Krop et al., 2012; Tolcher et al., 2012). Pan-Notch inhibition with GSIs is toxic because Notch signaling is crucial for the homeostasis of many tissues, such as the intestine(van Es et al., 2005; VanDussen et al., 2012). Apart from toxicity, another growing concern is that pan-NOTCH inhibitors could promote cancer. NOTCH has been implicated as a tumor suppressor in certain cancers, such as squamous cell and myeloid cancers(Klinakis et al., 2011; Wang et al., 2011). Thus, there is a critical need to identify the factors that preferentially amplify the oncogenic functions of the NOTCH pathway as opposed to its essential physiological functions. Targeting these factors may combat cancer cell growth while avoiding intolerable toxic effects.

Zmiz1 is a member of the Protein Inhibitor of Activated STAT (PIAS)-like family of coregulators. PIAS proteins do not bind DNA directly, but they bind and regulate other DNA-binding transcription factors(Shuai and Liu, 2005). Multiple murine mutagenesis

screens previously suggested that Zmiz1 is a Notch1 collaborator in T-ALL(Dupuy et al., 2005; Uren et al., 2008). The largest screen identified three genes as functional collaborators of Notch1 – *Lfng*, *Ikaros*, and *Zmiz1*. *Lfng* and *Ikaros* are well-established regulators of Notch1, but little is known about Zmiz1 and the Notch pathway. Zmiz1 was initially discovered as a coregulator of the androgen receptor(Sharma et al., 2003). It is widely and variably expressed with low levels in thymus(Sharma et al., 2003), but its expression is enriched in the earliest thymic precursors(Rakowski et al., 2013). We previously found that ZMIZ1 is variably expressed in human T-ALL and overexpressed in approximately 30% of patient samples (based on protein expression)(Rakowski et al., 2013). ZMIZ1 is co-expressed with activated NOTCH1 across a broad range of T-ALL oncogenomic subgroups. ZMIZ1 inhibition slows human T-ALL cell proliferation and/or sensitizes them to GSI(Rakowski et al., 2013)(data not shown).

In this study, we investigated the significance and mechanism of Zmiz1 in normal physiology and leukemia using mouse models. Similar to Notch, Zmiz1 was important for T-cell development and leukemogenesis. However, unlike Notch, Zmiz1 was not important for intestinal homeostasis or myeloid suppression. Zmiz1 directly interacted with Notch1 through an N-terminal tetratricopeptide repeat domain at a special class of Notch binding sites and selectively coregulated Notch1 transcriptional activity, particularly through the *Myc* enhancer. We here report that Zmiz1 is a direct Notch1 cofactor that heterogeneously regulates Notch target genes, which may have important implications for the precise control of Notch functions for a variety of applications.

Results

Zmiz1 has partially overlapping functions with Notch during thymopoiesis

We generated conditional *Zmiz1* knockout mice (*Zmiz1*$^{f/f}$) in which LoxP sites flank Exon 9 (see Supplemental Experimental Procedures). We crossed floxed mice to *Mx1Cre* transgenic mice to generate *Mx1CreZmiz1*$^{f/f}$ mice. We injected polyinosinic-polycytidylic acid (pIpC) to delete Zmiz1. At 8 weeks, deletion was generally >95% complete in the bone marrow (BM), >90% complete in the thymus, and ~80% complete in the spleen (Figure 1A). Deletion in the intestine was ~60% in the intestinal crypt and ~50% in full-thickness intestine.

We first examined the role of Zmiz1 in T-cell development. Notch1 signaling is required for Early Thymocyte Precursor (ETP) specification(Maillard et al., 2004; Radtke et al., 1999). Deletion of *Zmiz1* reduced thymus cellularity by ~4–5-fold compared to control mice (Figure 1B), but had no significant effect on BM or splenic cellularity (data not shown). Similar to deletion of *Notch1*, deletion of Zmiz1 resulted in reduced numbers of all thymic T-cell subsets (Figures S1A–I). There was no obvious block at any specific stage of development (data not shown). We saw no effects on peripheral T cells (Figures S1J and S1K). However, competitive transplant assays showed a 3- to 5-fold reduction in peripheral T cells generated by *Zmiz1*-deleted BM (Figures S2A–C and data not shown) and the defects were cell-autonomous (Figures S2F–L and data not shown). RT-PCR of double-negative 3 (DN3) cells showed that deletion of *Zmiz1* caused a significant ~4-fold reduction in transcripts of Notch target genes *Myc* and *Hes1* (Figure 1C). Interestingly, the transcripts of

other Notch target genes (*Dtx1*, *Il2ra*, and *Notch3*) were not significantly affected. These data suggest that Zmiz1 and Notch1 have converging roles in establishing ETP cells and regulating a subset of Notch1 target genes.

Unlike Notch, Zmiz1 is dispensable for myeloid suppression

Notch is important for suppressing myeloproliferation (Klinakis et al., 2011). In contrast, we found that Zmiz1 was dispensable for myeloid suppression (Figures S1L, S1M, S2D, S2E, S2Q–S). We did not observe myeloproliferation for >9 months after pIpC injection (data not shown). Notch signaling is dispensable for steady-state adult hematopoietic stem cell homeostasis(Maillard et al., 2008). Accordingly, hematopoietic stem/progenitor cell numbers were unaffected in Zmiz1-deficient mice (Figure S1N). Unlike Notch-deficient mice, which have no reported defects in the NK-lineage, we observed a ~2-fold loss of NK cell numbers (Figure S1O), modest cell-autonomous losses of B-cell subsets (Figures S2N–P and data not shown), and no accumulation of thymic B cells (Figures S1Q, S1R, S2M and data not shown). In the *Zmiz1*$^{\Delta Mx1Cre}$ mice, we did not observe effects on B cells (Figure S1S and data not shown), CD11c^{+} cells (Figure S1T), erythroid cells (Figures S1U, S1V, and data not shown), or platelets (Figure S1W). These data suggest that although Notch and Zmiz1 have similar functions in T cells, they have diverging functions outside of the T-cell lineage.

Deletion of *Zmiz1* induced transient goblet cell hyperplasia

In order to understand the role of Zmiz1 in intestinal homeostasis, we looked at Zmiz1 expression in the intestine. We observed similar, relatively low levels of Zmiz1 transcripts in murine thymus and intestinal crypt cells (data not shown). Notch and/or gamma-secretase inhibition in the intestine promotes globlet cell hyperplasia(van Es et al., 2005; VanDussen et al., 2012). However, we only observed a modest increase (~24%) in goblet cells 10 days after deletion of *Zmiz1* (Figures 1D and 1E) and these differences resolved by 8 weeks. The recovery of the intestine could not be explained by outgrowth of non-deleted cells (Figure 1A). To confirm that the recovery of the intestine was not due to the outgrowth of non-deleted cells, we generated mice with an intestinal-specific deletion using the *VilCreER*^{T2} transgene. *Zmiz1*$^{\Delta VilCreERT2}$ mice also did not generate secretory hyperplasia, suggesting that the initial increase seen in the *Zmiz1*$^{\Delta Mx1Cre}$ mice was a cell non-autonomous effect (Figures S2T–V). *Zmiz1*-deleted mice did not develop diarrhea or weight loss after >2 months of observation (data not shown). These data suggest a milder role for Zmiz1 than Notch in intestinal homeostasis.

Zmiz1 is important for Notch-induced T-ALL initiation and maintenance

To determine the significance of Zmiz1 in T-ALL initiation and maintenance, we used a well-established murine model of Notch1-induced T-ALL (Aster et al., 2000). Activating mutations in *NOTCH1*, such as L1601PΔP, are a defining feature of human T-ALL. We transduced *Mx1CreZmiz1*$^{f/f}$ BM stem cells with L1601PΔP and transplanted these cells into recipient mice. To test the effect of *Zmiz1* deletion on T-ALL initiation, we injected recipient mice with pIpC at 1 week after transplant (Figure 2A). As expected, control mice developed circulating preleukemic CD4^{+}CD8^{+} double-positive (DP) T cells. In contrast,

deletion of *Zmiz1* caused a ~7-fold reduction in DP T-cell frequency (Figures 2B and 2C). DP T cells are preleukemic, low-proliferative, and correlate with strength of Notch signaling(Chiang et al., 2008; Li et al., 2008). L1601PΔP induced T-ALL in 30% of control mice, but none of the *Zmiz1*-deleted mice (Figure 2D). When T-ALL was induced with the stronger ΔEGFΔLNRΔP allele(Chiang et al., 2006), deletion of *Zmiz1* caused a significant 1.6-fold reduction in DP T-cell frequency at 4 weeks after transplant (Figures 2E and 2F). The median survival was 55 days longer in *Zmiz1*-deleted mice than in controls (Figure 2G). These data suggest that Zmiz1 is important for initiation of Notch-induced T-ALL.

To determine the effect of *Zmiz1* deletion on T-ALL maintenance, we first transduced *Mx1CreZmiz1*$^{f/f}$ BM stem cells with ΔEGFΔLNRΔP and transplanted these cells into recipient mice. The white blood cell counts began to climb above 100K/μl at ~5 weeks post injection, indicative of leukemia. We injected pIpC to delete *Zmiz1* after leukemia was established and 2–3 weeks later observed a ~2-fold reduction of peripheral DP T-cell frequency in deleted mice relative to control mice (Figures 2H and 2I). The frequency of splenic DP T cells and absolute numbers of leukemic infiltration into BM, lymph nodes, spleen and thymus were also reduced in *Zmiz1*-deleted mice (compare Figure S3A to S3B, data not shown). Deletion of *Zmiz1* significantly prolonged survival and reduced the fraction of mice succumbing to T-ALL (Figures 2J and S3C). Since Zmiz1 appeared to be important for T-ALL leukemogenesis, we suspected that the T-ALL cells that deleted Zmiz1 would proliferate more slowly than cells that escaped Cre-mediated recombination. To test this possibility, we transplanted primary tumors into secondary recipients (Figures S3D and S3E). If deletion of *Zmiz1* impaired T-ALL expansion, then we would expect that the secondary tumors would be dominated by cells that escaped *Zmiz1* deletion. Thus, we compared the deletion efficiency of tumors derived from primary and secondary transplanted mice. Whereas the frequency of deletion ranged from 18–26% in the primary tumors, the frequency of deletion in the secondary tumors dropped to 0–2% (Figure S3F). Thus, *Zmiz1*-deleted leukemic cells appeared to have a proliferative disadvantage compared to *Zmiz1*-widtype leukemic cells. These data suggest that Zmiz1 is important for maintenance of Notch-induced T-ALL.

The N-terminal domain (NTD) is critical for Zmiz1 to function as a Notch collaborator

To investigate potential toxicities of targeting Zmiz1, we deleted *Zmiz1* ubiquitously using *Rosa26-CreER*^{T2}. Deletion did not cause observable toxicity or weight changes (Figures S3G and S3H). We next sought to understand the mechanistic basis for the “Notch-like” phenotypes in Zmiz1-deficient mice with the objective of identifying a strategy to target Zmiz1. Given that Zmiz1 appeared to regulate *Myc* strongly in developing T cells, we focused on the ability of Zmiz1 to enhance Notch-induced *Myc* transcription(Rakowski et al., 2013). As Zmiz1 cannot directly bind DNA, we hypothesized that Zmiz1 binds a transcription factor. To test this, we first identified the domain that Zmiz1 uses to induce *Myc* transcription. Using PHYRE and BLAST to structurally predict the boundaries of Zmiz1 domains, we created mutants lacking individual domains of Zmiz1 (Figure 3A). These mutants were transduced into 8946 cells to test their ability to drive Myc expression in collaboration with L1601PΔP. 8946 is a murine T-ALL cell line that is dependent on a tet-regulated human *MYC* transgene and expresses undetectable levels of ICN1 and very low

levels of Zmiz1 (data not shown). Upon addition of doxycycline, the *MYC* transgene is downregulated and the cells die. However, if the cells are co-transduced with L1601PΔP and Zmiz1, murine Myc is expressed, and the cells proliferate. Deletion of amino acids 1–250 (ΔN) or the transcriptional activation domain (ΔTAD) abolished the ability of Zmiz1 to induce *Myc* transcripts and drive proliferation (Figures 3B–D). PHYRE predicted that amino acids 1–120 ("NTD") would be structured while amino acids 121–250 ("N2") would be disordered. Deletion of NTD (ΔNTD) but not N2 (ΔN2) abolished the ability of Zmiz1 to induce *Myc* transcription or drive cell proliferation (Figures 3E–G). The N and TAD domains were sufficient to induce *Myc* transcription and drive cell proliferation (Figures 3H–J). As Zmiz2 lacks a domain homologous to the NTD, we predicted that Zmiz2 could not substitute for Zmiz1. Accordingly, high levels of Zmiz2 only weakly induced *Myc* and failed to drive proliferation (Figures 3K–N). We next transfected U2OS cells with a Notch-dependent reporter construct together with Zmiz1 expression constructs and intracellular forms of Notch1. U2OS is an osteosarcoma cell line with low levels of active Notch. Zmiz1, but not ΔNTD, enhanced Notch-driven reporter activity (Figures 4A and 4B). Further, ectopic expression of the combined N and TAD domains of Zmiz1 were sufficient to rescue the proliferation of human T-ALL cells that were transduced with shZMIZ1 (Figure 4C). These data suggest an NTD-dependent mechanism of Zmiz1 action that is independent of MIZ domain functions.

The N-terminal domain (NTD) of Zmiz1 is a tetratricopeptide repeat (TPR) domain that directly interacts with the RAM domain of Notch1

In order to understand the mechanism of NTD function we solved its three-dimensional structure (Figure 4D). Our structural analyses identified the NTD as containing tandem tetratricopeptide repeats (TPR). TPR domains mediate protein-protein interactions in hundreds of proteins (Zeytuni and Zarivach, 2012). We will henceforth refer to the NTD as "TPR." In order to identify proteins interacting with TPR, we performed affinity purification mass spectrometry (MS) of 8946 cells transduced with FLAG-tagged TPR as the bait. Our screen identified 14 known transcriptional regulators that were differentially immunoprecipitated with the TPR bait compared to control vector (Figure 4E). The top ranked hit was Notch1, and the third and fifth ranked hits were the other two components of the core Notch1 complex (Maml1 and Rbpj respectively). These data suggest that Zmiz1 interacts with the Notch1 complex through the TPR domain.

Our MS results were unexpected since previous experiments did not identify an interaction between Notch1 and Zmiz1(Rakowski et al., 2013). However, co-immunoprecipitation (co-IP) studies using optimized conditions revealed that FLAG-Zmiz1 interacted with ICN1 and endogenous Rbpj in Notch-transduced 8946 cells (Figures 5A and 5B). The FLAG-Zmiz1 construct was expressed at levels comparable to endogenous ZMIZ1 in CEM/SS human T-ALL cells (Figure S4A). TPR was both sufficient (Figure 5C) and necessary (Figure 5D) for the interaction. ZMIZ1 interacted with ICN1 and RBPJ in human T-ALL cells (Figures 5E and 5F) and in reverse co-IPs (Figure 5G). We were unable to validate interactions between TPR and other possible partners in Figure 4E (data not shown). Our use of forward and reverse co-IP detected interactions with endogenous proteins in multiple cell lines and yielded consistent results, supporting the notion that Notch1 interacts with Zmiz1.

We next tested whether Zmiz1 interacted directly with the RAM-ANK domain of Notch1 (Figure 6A). GST pull-down assay showed a direct interaction between RAM-ANK and TPR (Figure 6B). In order to confirm direct binding, we mixed ^{15}N-labeled untagged TPR with untagged RAM-ANK. We observed shifts for number of peaks in the NMR spectrum of TPR, which indicated direct binding (Figures 6C–E). In particular, we observed a strong broadening of the W38 peak of TPR (compare Figure 6F to 6G). RAM but not ANK retained binding to TPR (compare Figure 6H to 6I). ANK forms a transcriptionally active complex with Rbpj and Maml. If Zmiz1 interacted with RAM, but not ANK, then Zmiz1 should not enhance ANK transcriptional activity. Accordingly, Zmiz1 did not significantly enhance ANK-driven transcription (Figure 6J). Finally, given potential toxicity of targeting all Zmiz1 functions, we tested the feasibility of targeting just the TPR-Notch1 interaction. Accordingly, the TPR alone and a TPR-DsRed fusion protein acted as dominant-negative inhibitors in the Notch reporter assay (Figures 6K, 6L, and S4B). Furthermore, transduction of the TPR-DsRed inhibited T-ALL proliferation (Figure 6M). These data are indicative of direct binding between the RAM domain of Notch1 and the TPR domain of Zmiz1.

Zmiz1 selectively co-binds a subset of Notch regulatory sites

Our observation of a direct interaction between Zmiz1 and Notch1 led us to consider the possibility that these proteins interacted at the chromatin level. We were previously unable to perform ChIP using the FLAG or Zmiz1 antibodies(Rakowski et al., 2013). Thus, we used an HA antibody to recognize HA-tagged Zmiz1 (HA-Zmiz1). The HA-Zmiz1 construct was expressed at levels comparable to endogenous ZMIZ1 in Jurkat T-ALL cells (Figure S4A). We performed ChIP-Seq in 8946 cells transduced with HA-Zmiz1 and Notch1. We identified 4,897 Zmiz1 (HA) peaks, 20,485 Rbpj peaks, and 383 ICN1 peaks with FDR<0.01 (Figure 7A; Figures S4C–E for distributions). A large majority (75%) of ICN1/Rbpj peaks overlapped with Zmiz1 (HA) peaks (273 peaks). 27% of ICN1 peaks with overlapping Rbpj but not Zmiz1 (HA) peaks were distributed to promoters (Figure 7B, Table S1). In contrast, only 6% of ICN1 peaks with overlapping Rbpj and Zmiz1 (HA) peaks were distributed to promoters (Figure 7C, Table S2). Thus, similar to dynamic Notch1 sites and Ets1 sites(Wang et al., 2014), Notch1 sites that were co-bound with Zmiz1 were less frequently found at promoters than all Notch1 sites. Consistent with the notion that ICN1 binds Rbpj, the size of ICN1 signals correlated with the size of Rbpj signals (Figure S4F, R=0.44). In contrast, Zmiz1 appeared to interact with ICN1 only at select sites at the chromatin. Accordingly, the size of Zmiz1 (HA) signals had moderate correlation with the size of Rbpj signals (Figure S4G, R=0.31) and ICN1 signals (Figure S4H, R=0.37)(Figure S4I). Similar to Rbpj and ICN1 peaks, Zmiz1 (HA) peaks were associated with activating H3K27ac, H3K4me1, and H3K4me3 chromatin marks and were devoid of repressive H3K27me3 marks (Figure S4J–L). We identified co-occupancy of Zmiz1 (HA), ICN1, and Rbpj peaks at enhancers in previously identified Notch binding sites (Figure 7D and Figure S5A). Zmiz1 bound the distal 3′ *Myc* enhancer, which was recently found to be crucial for T-lineage specific, Myc expression, and maintenance of Notch-induced T-ALL(Herranz et al., 2014; Yashiro-Ohtani et al., 2014). These Zmiz1 binding sites were validated using conventional ChIP (Figure S5B). These data are consistent with selective binding of Zmiz1 at a subset of ICN1 and Rbpj-regulated sites.

Our results seemed to contradict our previous data suggesting that *Myc* was an indirect target of Zmiz1(Rakowski et al., 2013). Previously, we showed that a chimeric protein (Zmiz1-ER) consisting of Zmiz1 fused to the ligand-binding domain of the estrogen receptor (ER) is unable to drive Myc transcription in the presence of cycloheximide (CHX). We considered the possibility that the ER domain was altering Zmiz1 function since we had fused it directly to the C-terminal end of the TAD of Zmiz1. We thus constructed a second chimeric protein called Zm(ER)iz1 in which the ER was placed in the middle of Zmiz1. Zm(ER)iz1 could drive Myc expression even in the presence of CHX (Figures S5C and S5D). This data supports our model that Zmiz1 binds ICN1, which directly regulates *Myc*.

Zmiz1 and Notch1 cooperatively recruit each other to chromatin through the TPR domain

Our observation of a direct interaction between ICN1 and Zmiz1 led us to consider the possibility that ICN1 and Zmiz1 cooperatively recruited each other to chromatin. Our model predicts that GSI would interfere with Zmiz1 binding by depleting ICN1. Accordingly, GSI significantly reduced Zmiz1 binding at Notch-dependent sites but not at negative control sites (Figure S5E). To further show cooperative binding on chromatin, we generated four 8946 cell lines in which L1601P or Zmiz1 were expressed alone or in combination. We then performed RNA-Seq and ChIP at the Notch-dependent *Myc* enhancer (Figure S6A). Since L1601P generates low levels of ICN1, we relied on the more sensitive Rbpj antibody to detect the Notch1 complex. The addition of L1601P increased Zmiz1 (HA) binding to the *Myc* enhancer (Figure S6B, compare 2nd and 4th columns), but not to a control site (Figure S6C). Conversely, the addition of Zmiz1 increased Rbpj binding to the *Myc* enhancer (Figure S6D, compare 3rd and 4th columns), but not to a control site (Figure S6E). Further, addition of Zmiz1 slightly increased the activating H3K27ac mark (Figure S6F, compare 3rd and 4th columns) at the *Myc* enhancer, but not at a control site (Figure S6G). Our model predicts that deletion of the TPR domain (ΔTPR) would impair recruitment of Zmiz1 or Rbpj. Accordingly, L1601P had no effect on the binding of the ΔTPR mutant (Figure S6H, compare 3rd and 6th columns). Further, ΔTPR had no effect on Rbpj binding (Figure S6I, compare 4th and 6th columns), on the activating H3K27ac mark (Figure S6J, compare 4th and 6th columns), or on the repressive H3K27me3 mark (Figure S6K, compare 4th and 6th columns). In contrast, wildtype Zmiz1 reduced the repressive H3K27me3 mark (Figure S6K, compare 4th and 5th columns). Our data suggest that Zmiz1 and Notch1 cooperatively recruit each other to chromatin through direct interaction via the TPR resulting in a slight increase in activating histone marks and decrease of repressive histone marks.

“Zmiz1-independent” Notch1/Rbpj sites

Due to the high stringency of the MACS2 algorithm, the percentage of ICN1/Rbpj sites that overlap with Zmiz1 sites was likely higher than 75%. However, we identified ICN1/Rbpj sites where ChIP could not detect Zmiz1 (HA) binding (examples in Figure S6L, compare 2nd and 3rd columns). Here the addition of Notch1 but not Zmiz1 significantly increased binding of ICN1 or Rbpj (Figures S6M and S6N).

Zmiz1 selectively regulates a subset of Notch1 target genes, particularly Myc, in murine and human T-ALL

Our ChIP-Seq data led us to hypothesize that Zmiz1 regulates only a subset of Notch1 target genes. To investigate this, we performed RNA-Seq on the 8946 cells transduced with L1601P and/or Zmiz1 (Figure S6A). We first identified all target genes that were regulated by Notch1 (Figure 7E). We next determined the fold change for each gene upon further addition of Zmiz1. The Notch1-induced target gene that was most strongly upregulated by the further addition of Zmiz1 was clearly *Myc* (purple circle, Figure 7E). About 43% of Notch1-induced target genes were co-regulated by Zmiz1 (Figure S7A, Table S3). We observed a small, significant induction of endogenous Zmiz1 (~17%) by Notch1 (data not shown). These data show that Zmiz1 selectively regulates a subset of Notch1 target genes with strong amplification of the *Myc* oncogene.

We next considered the possibility that this same selectivity occurs in human T-ALL. In human CEM-type T-ALL cells, ~7% of NOTCH target genes were also ZMIZ1 target genes (Figure S7B, Table S4). We identified ZMIZ1-regulated genes in proliferation-type pathways using MSigDB gene lists (Figure S7C). Among the NOTCH-dependent ZMIZ1-regulated genes were *MYC*, *IL7R*, and *HES1* (Figures S7C, green highlights, and S7D). *MYC*, *IL7R*, and *HES1* are important direct NOTCH1 target genes in T-ALL. The combination of GSI and shZMIZ1 downregulated MYC transcripts more effectively than GSI or shZMIZ1 individually (Figure S7E and S7F; ANOVA analysis in Figure S7G). The effectiveness of the combination was also seen on MYC protein (Figure S7H, compare 2nd lane to 4th and 6th lanes). These data suggest that ZMIZ1 selectively coregulates *MYC* in human T-ALL cells similar to murine T-ALL. The importance of ZMIZ1 in non-NOTCH pathways was suggested by the more profound effect of Zmiz1 deletion on survival than on frequencies of Notch-induced DP T cells (compare Figure 2G to Figure 2F). To further evaluate this, we silenced the top 4 genes induced by ZMIZ1 but not NOTCH in Figure S7C (grey highlights). Knockdown suppressed proliferation (Figures S7I–L). These data suggest that NOTCH-independent ZMIZ1-regulated genes have functional significance.

Zmiz1 binds a special class of Notch-regulatory sites

To understand the selectivity of Zmiz1, we considered the possibility that Zmiz1 may regulate genes based on the number or strength of binding sites. However, we found only modestly higher peak numbers and sizes of Zmiz1 but not ICN1/Rbpj in genes positively regulated by Zmiz1 (data not shown). We next considered the possibility that there was a Notch1-independent transcription factor that recruited Zmiz1 to chromatin and therefore performed de novo motif analysis (Figure 7F). At Type A sites, ICN1 and Rbpj were bound, but Zmiz1 was not bound. At Type B sites, ICN1, Rbpj, and Zmiz1 were bound. At Type C sites, Zmiz1 was bound, but Rbpj and ICN1 were not bound. Rbpj was the most highly and significantly enriched motif at Type A and Type B sites, but not Type C sites. Basic Helix-Loop-Helix (bHLH), Tcf, Runx, and Ets motifs were the next most highly and significantly enriched motifs at Type B sites and the most highly and significantly enriched motifs at Type C sites (P<1E-13). These motifs were not enriched at Type A sites. These data suggest that Zmiz1 homes to sites where bHLH, Tcf, Runx, and Ets factors bind even when ICN1 is absent and avoids sites where these factors do not bind even when ICN1 is present.

Accordingly, ETS1 co-bound NOTCH-regulatory sites in the 3′ *MYC* enhancer and other loci (Figure 7G). Furthermore, Zmiz1 bound Ets1 through a TPR-independent mechanism (Figure 5D). The strength of ICN1/Rbpj binding was not a major factor in determining binding of Zmiz1 (Figure 7H). These data suggest that the selectivity of Zmiz1 for certain Notch1 target genes but not others may be controlled in part by its preference for a special class of Notch regulatory sites.

Discussion

The challenge facing the development of NOTCH-directed therapeutics is to selectively target the functions of NOTCH in cancer and preserve the functions of NOTCH in normal tissue homeostasis and tumor suppression. A theoretical strategy is to selectively target the gene regulatory functions of the core NOTCH complex. On one hand, some direct NOTCH cofactors, such as MAML, may be non-selective. Inhibiting these nonselective cofactors would homogeneously inhibit NOTCH functions and would be predicted to cause the same intolerable toxicities as GSI. On the other hand, there might exist a pool of context-dependent direct NOTCH cofactors that heterogeneously regulate ICN. If so, it might be possible to precisely control NOTCH signaling with acceptable toxicities by targeting specific protein-protein interactions. The challenge is that the direct transcriptional regulators of the core NOTCH complex are poorly understood. ICN1 recruits the histone acetyltransferases Pcaf, Gcn5, and p300/CBP(Kurooka and Honjo, 2000; Oswald et al., 2001). Maml1 recruits p300/CBP(Fryer et al., 2002). MS analysis revealed several proteins that associated with the NOTCH core complex(Yatim et al., 2012). However, it is unclear whether these regulators are recruited directly or are selective for certain NOTCH target genes.

We found that Zmiz1, through a previously unappreciated TPR domain, directly engaged ICN1 to selectively regulate Notch1 target genes. By “selective,” we mean that Zmiz1 regulated ~43% of Notch1 target genes and co-bound ~75% of Notch1/Rbpj binding sites. This selectivity was at least in part due to the preference of Zmiz1 for a special class of Notch binding site. However, as is the case for other transcription factors like NOTCH1(Wang et al., 2014), ChIP-Seq revealed that Zmiz1 binding sites greatly outnumber regulated genes. Thus, there are other determinants for the selectivity other than Zmiz1 binding. Zmiz1 target genes included Notch target genes important for T-cell development and leukemia such as *Myc* and *Hes1*. Selective loss of Notch target genes may explain why Zmiz1-deficient mice displayed the loss of ETP cells, but not the expansion of thymic B cells or the selective loss of marginal zone B cells that is seen in Notch-deficient mice. Accordingly, Hes1-deficient mice do not accumulate thymic B cells or show selective loss of marginal zone B cells (Wendorff et al., 2010). However, additional experiments are needed to test this more thoroughly. Additional in vivo studies are also needed to comprehensively identify and functionally validate the critical target genes of Zmiz1 during the biologically distinct processes of ETP specification, leukemia initiation, and leukemia maintenance using comparative gene expression profiling of Notch-deficient and Zmiz1-deficient cells followed by in vitro and in vivo functional validation. We expect many challenges in these endeavors as the Notch target genes important for these processes are still debated and incompletely understood despite several years since the first reports of T-

cell defects in Notch1-deficient mice(Radtke et al., 1999) and T-ALL in Notch1-activated mice(Pear et al., 1996).

The selectivity of Zmiz1 for certain Notch1 target genes may be clinically relevant when considering potential toxicities of Zmiz1-directed therapy. For example, in contrast to mouse models of pan-Notch deficiency, our Zmiz1-deficient mice did not develop sustained or severe gut toxicity, myeloproliferative disease, or weight loss. While this was reassuring, our mice displayed defects not found in Notch-deficient mice. Thus, we are mindful of the potential importance of Notch-independent functions of Zmiz1. In this regard, we identified an interaction of Zmiz1 with Ets1. As Ets1-deficient mice have defects in T-cell, B-cell and NK-cell development(Barton et al., 1998; Bories et al., 1995; Muthusamy et al., 1995), it is possible that combined partial alterations in Notch and Ets1 functions may be contributing to the defects in Zmiz1-deficient mice. Testing this possibility will be challenging, but could be done by mapping the critical amino acids at the interface with each binding partner using a combination of mutagenesis and biophysical methods such as x-ray crystallography and NMR. These data would enable us to rationally design well-controlled small molecule, mutagenesis, and dominant-negative strategies to selectively disrupt one interaction while preserving the other and then observing effects on lymphopoiesis, leukemia initiation, leukemia maintenance, and target gene expression. To reduce toxicity, it may be important to specifically target the Notch-dependent functions of Zmiz1. As the TPR is dispensable for the Zmiz1-Ets1 interaction and as we have not validated TPR interactions with other potential partners in Figure 4E, we predict that targeting the TPR-Notch1 interaction may preserve Zmiz1 interactions with other binding partners. This would likely be less toxic than inhibiting all Zmiz1 functions. Accordingly, we showed that the TPR domain acted as a dominant-negative and suppressed T-ALL cell growth.

Our findings suggest that the view of the lone ICN1 complex sitting on chromatin and driving gene expression robustly through a repetitive inflexible mechanism at every target gene may be outdated. This view is based on experiments using very strong, but artificial alleles (e.g. NICD1 or ICN1). However, we previously found that the mutated *NOTCH1* alleles in human samples vary in signal strength in several assays, but in general are much weaker than ICN1(Chiang et al., 2008). We propose a model, based on experiments using the weaker *NOTCH1* alleles commonly found in leukemia, that views the core NOTCH complex as intrinsically weak. It specifies gene expression, but relies on direct contact with transcriptional cofactors to amplify its functions. This model is consistent with recent ChIP-Seq experiments showing that certain transcription factors (e.g. RUNX1, ETS1, GABPA, and Ikaros) converge on a subset of NOTCH-regulated enhancers(Wang et al., PNAS, 2011; Geimer et al., Science Signaling, 2014; Wang et al., 2014). Although none of these factors are known to bind NOTCH directly, these data raise the possibility that direct NOTCH1 cofactors could similarly converge on ICN1. In T cells, we propose that NOTCH1 relies on ZMIZ1 to selectively amplify an important oncogenic subset of NOTCH1 signals (e.g. *MYC*) by direct regulation and possibly recruitment to an even larger transcriptional complex. This may offer the opportunity to combat T-ALL growth with NOTCH-directed therapy with acceptable adverse effects. We here report the discovery of a direct and selective cofactor of NOTCH1, which has promising translational potential as precise

control of NOTCH signals may treat conditions of T-cell deficiency, immune dysregulation, and cancer.

Experimental Procedures

Mice

4–8 week old C57BL/6 (CD45.2$^+$) mice and C57BL/6.Ly5.2 (B6-SJL, CD45.1$^+$) mice were obtained from Taconic and NCI/Charles River respectively. Experiments were performed according to NIH guidelines with approved protocols from the IACUC at the University of Michigan (Permit # PRO00005826). *Zmiz1*$^{f/f}$ mice were generated from ES cells obtained from EUCOMM (HEPD0641-2-B09). These ES cells are on the C57BL/6 Taconic background and contain an Exon 9 of *Zmiz1* that is flanked by two LoxP sites

Cell lines

Jurkat were provided by Jon Aster. CEM/SS were provided by Katherine Collins. 8946 and CUTTL1 were provided by Warren Pear and Adolfo Ferrando. LOUCY.2, a subclone of LOUCY, were provided by Uptal Dave. P12.2, a subclone of P12, and other T-ALL cell lines were provided by Andrew Weng. U2OS cells were provided by Chris Canman.

Antibodies

Antibodies used were as follows: ICN1 (Cell Signaling Technology, 2421), Rbpj (5313, Cell Signaling Technology), FLAG (F1804, Sigma), HA (3725, Cell Signaling Technology), β-actin (A5316, Sigma), MYC (D84C2; Cell Signaling Technology), and ZMIZ1 (AP6236a, Abgent). Antibodies for ChIP-Seq are as follows: H3K4me3 (Millipore, 07-473); H3K4me1 (Abcam, ab8895); H3K27me3 (Millipore #07-449); H3K27ac (Abcam, ab4729); HA (Abcam, ab9110, 2.5ug); mouse IgG isotype control (Cell Signaling Technology, 5315s); rabbit IgG isotype control (Cell Signaling Technology, 2729); Rbpj (Cell Signaling Technology, 5313); ICN1 (Cell Signaling Technology, 4147s).

Protein identification by LC-Tandem mass spectrometry

8946 cells were transduced with either the NGFR vector alone or FLAG-TPR. Proteins were separated by SDS-PAGE and digested with trypsin. Resulting peptides were resolved and directly introduced in to an ion-trap mass spectrometer (LTQ XL, ThermoFisher).

Crystallization and structure determination

Crystals of SeMet substituted ZMIZ1 TPR were grown by using the sitting-drop vapor diffusion method at 4°C. Diffraction data was collected on a SeMet substituted crystal at the Advanced Photon Source at LS-CAT beam line 21-ID-D. The final structure was refined to 1.7Å resolution and crystallographic R_{work} and R_{free} were 15.84% and 20.44%, respectively. The coordinates for the TPR domain were deposited in PDB under the code 5AIZ.

NMR

^{15}N-labeled TPR was expressed and purified using size exclusion chromatography. Samples for NMR studies contained 50 μM ^{15}N TPR in 50 mM Tris, pH 7.5 and 50 mM NaCl buffer. All NMR spectra were measured using Bruker 600 MHz spectrometer at 25°C.

ChIP-Seq/RNA-Seq

The ChIP DNA was prepared from 8946 cells transduced with activated Notch1 and Zmiz1. Histone mark samples were prepared using formaldehyde crosslinking. Other samples were prepared using DSG with formaldehyde crosslinking. The sequencing library was prepared using the Illumina Hi-Seq library preparation kit. For RNA-Seq, 8946 cells were transduced in triplicate with (1) MigR1 and NGFR empty vectors; (2) MigR1-L1601P and NGFR empty vector; (3) MigR1 and Zmiz1-NGFR; or (4) MigR1-L1601P and Zmiz1-NGFR. RNA samples with RINs of 8 or greater were prepped using the Illumina TruSeq mRNA Sample Prep v2 kit (Catalog #s RS-122-2001, RS-122-2002) (Illumina, San Diego, CA). Final libraries were sequenced on a 50 cycle single end on a HiSeq 2000 (Illumina) in High Output mode using version 3 reagents according to manufacturer's protocols. The reads were mapped to mm10 assembly using Bowtie (version 0.12.7) to generate uniquely mapped alignments.

Deposition of sequences

The sequencing data was deposited in the Gene Expression Omnibus with accession number GSE66147.

Supplementary Material

Refer to Web version on PubMed Central for supplementary material.

Acknowledgments

We thank Warren Pear, Andrew Weng, Adolfo Ferrando, Raphael Kopan, Jon Aster, Stephen Blacklow, Kelly Arnett, Venkatesha Basrur, Weisheng Wu, Manjusha Pande, Jeanne Geskes, Choi Li, Jordan McHugh, Amanda Day, Paula Jeon, Zijie Sun, Maria Figueroa, and Cailin Collins for invaluable assistance. M.Y.C. was supported by the American Cancer Society (RSG-11-189-01-TBG), Elisa U. Pardee Foundation, Rally Foundation for Childhood Cancer Research, Vs. Cancer Foundation, Bear Necessities Pediatric Cancer Foundation, Concern Foundation, and the American Society of Hematology. Other support was provided to R.K. (P30-CA46592), N.P. (T32-CA009676-22), I.M. (R01-AI091627), and L.S. (R01-DK078927).

References

Aster JC, Xu L, Karnell FG, Patriub V, Pui JC, Pear WS. Essential roles for ankyrin repeat and transactivation domains in induction of T-cell leukemia by Notch1. Mol Cell Biol. 2000; 20:7505–7515. [PubMed: 11003647]

Barton K, Muthusamy N, Fischer C, Ting CN, Walunas TL, Lanier LL, Leiden JM. The Ets-1 transcription factor is required for the development of natural killer cells in mice. Immunity. 1998; 9:555–563. [PubMed: 9806641]

Bories JC, Willerford DM, Grevin D, Davidson L, Camus A, Martin P, Stehelin D, Alt FW. Increased T-cell apoptosis and terminal B-cell differentiation induced by inactivation of the Ets-1 proto-oncogene. Nature. 1995; 377:635–638. [PubMed: 7566176]

Chiang MY, Xu L, Shestova O, Histen G, L'Heureux S, Romany C, Childs ME, Gimotty PA, Aster JC, Pear WS. Leukemia-associated NOTCH1 alleles are weak tumor initiators but accelerate K-ras-initiated leukemia. Journal of Clinical Investigation. 2008; 118:14.

Chiang MY, Xu ML, Histen G, Shestova O, Roy M, Nam Y, Blacklow SC, Sacks DB, Pear WS, Aster JC. Identification of a conserved negative regulatory sequence that influences the leukemogenic activity of NOTCH1. Mol Cell Biol. 2006; 26:6261–6271. [PubMed: 16880534]

Dupuy AJ, Akagi K, Largaespada DA, Copeland NG, Jenkins NA. Mammalian mutagenesis using a highly mobile somatic Sleeping Beauty transposon system. Nature. 2005; 436:221–226. [PubMed: 16015321]

Fryer CJ, Lamar E, Turbachova I, Kintner C, Jones KA. Mastermind mediates chromatin-specific transcription and turnover of the Notch enhancer complex. Genes Dev. 2002; 16:1397–1411. [PubMed: 12050117]

Herranz D, Ambesi-Impiombato A, Palomero T, Schnell SA, Belver L, Wendorff AA, Xu L, Castillo-Martin M, Llobet-Navas D, Cordon-Cardo C, et al. A NOTCH1-driven MYC enhancer promotes T cell development, transformation and acute lymphoblastic leukemia. Nat Med. 2014; 20:1130–1137. [PubMed: 25194570]

Klinakis A, Lobry C, Abdel-Wahab O, Oh P, Haeno H, Buonamici S, van De Walle I, Cathelin S, Trimarchi T, Araldi E, et al. A novel tumour-suppressor function for the Notch pathway in myeloid leukaemia. Nature. 2011; 473:230–233. [PubMed: 21562564]

Krop I, Demuth T, Guthrie T, Wen PY, Mason WP, Chinnaiyan P, Butowski N, Groves MD, Kesari S, Freedman SJ, et al. Phase I pharmacologic and pharmacodynamic study of the gamma secretase (Notch) inhibitor MK-0752 in adult patients with advanced solid tumors. J Clin Oncol. 2012; 30:2307–2313. [PubMed: 22547604]

Kurooka H, Honjo T. Functional interaction between the mouse notch1 intracellular region and histone acetyltransferases PCAF and GCN5. J Biol Chem. 2000; 275:17211–17220. [PubMed: 10747963]

Li X, Gounari F, Protopopov A, Khazaie K, von Boehmer H. Oncogenesis of T-ALL and nonmalignant consequences of overexpressing intracellular NOTCH1. Journal of Experimental Medicine. 2008; 205:2851–2861. [PubMed: 18981238]

Maillard I, Koch U, Dumortier A, Shestova O, Xu L, Sai H, Pross SE, Aster JC, Bhandoola A, Radtke F, et al. Canonical notch signaling is dispensable for the maintenance of adult hematopoietic stem cells. Cell Stem Cell. 2008; 2:356–366. [PubMed: 18397755]

Maillard I, Weng AP, Carpenter AC, Rodriguez CG, Sai H, Xu L, Allman D, Aster JC, Pear WS. Mastermind critically regulates Notch-mediated lymphoid cell fate decisions. Blood. 2004; 104:1696–1702. [PubMed: 15187027]

Muthusamy N, Barton K, Leiden JM. Defective activation and survival of T cells lacking the Ets-1 transcription factor. Nature. 1995; 377:639–642. [PubMed: 7566177]

Oswald F, Tauber B, Dobner T, Bourteele S, Kostezka U, Adler G, Liptay S, Schmid RM. p300 Acts as a transcriptional coactivator for mammalian notch-1. Mol Cell Biol. 2001; 21:7761–7774. [PubMed: 11604511]

Pear WS, Aster JC, Scott ML, Hasserjian RP, Soffer B, Sklar J, Baltimore D. Exclusive development of T cell neoplasms in mice transplanted with bone marrow expressing activated Notch alleles. J Exp Med. 1996; 183:2283–2291. [PubMed: 8642337]

Radtke F, Wilson A, Stark G, Bauer M, van Meerwijk J, MacDonald HR, Aguet M. Deficient T cell fate specification in mice with an induced inactivation of Notch1. Immunity. 1999; 10:547–558. [PubMed: 10367900]

Rakowski LA, Garagiola DD, Li CM, Decker M, Caruso S, Jones M, Kuick R, Cierpicki T, Maillard I, Chiang MY. Convergence of the ZMIZ1 and NOTCH1 pathways at C-MYC in acute T lymphoblastic leukemias. Cancer Research. 2013; 73:930–941. [PubMed: 23161489]

Sharma M, Li X, Wang Y, Zarnegar M, Huang CY, Palvimo JJ, Lim B, Sun Z. hZimp10 is an androgen receptor co-activator and forms a complex with SUMO-1 at replication foci. EMBO J. 2003; 22:6101–6114. [PubMed: 14609956]

Shuai K, Liu B. Regulation of gene-activation pathways by PIAS proteins in the immune system. Nat Rev Immunol. 2005; 5:593–605. [PubMed: 16056253]

Tolcher AW, Messersmith WA, Mikulski SM, Papadopoulos KP, Kwak EL, Gibbon DG, Patnaik A, Falchook GS, Dasari A, Shapiro GI, et al. Phase I study of RO4929097, a gamma secretase inhibitor of Notch signaling, in patients with refractory metastatic or locally advanced solid tumors. J Clin Oncol. 2012; 30:2348–2353. [PubMed: 22529266]

Uren AG, Kool J, Matentzoglu K, de Ridder J, Mattison J, van Uitert M, Lagcher W, Sie D, Tanger E, Cox T, et al. Large-scale mutagenesis in p19(ARF)- and p53-deficient mice identifies cancer genes and their collaborative networks. Cell. 2008; 133:727–741. [PubMed: 18485879]

van Es JH, van Gijn ME, Riccio O, van den Born M, Vooijs M, Begthel H, Cozijnsen M, Robine S, Winton DJ, Radtke F, et al. Notch/gamma-secretase inhibition turns proliferative cells in intestinal crypts and adenomas into goblet cells. Nature. 2005; 435:959–963. [PubMed: 15959515]

VanDussen KL, Carulli AJ, Keeley TM, Patel SR, Puthoff BJ, Magness ST, Tran IT, Maillard I, Siebel C, Kolterud A, et al. Notch signaling modulates proliferation and differentiation of intestinal crypt base columnar stem cells. Development. 2012; 139:488–497. [PubMed: 22190634]

Wang H, Zang C, Taing L, Arnett KL, Wong YJ, Pear WS, Blacklow SC, Liu XS, Aster JC. NOTCH1-RBPJ complexes drive target gene expression through dynamic interactions with superenhancers. Proc Natl Acad Sci U S A. 2014; 111:705–710. [PubMed: 24374627]

Wang NJ, Sanborn Z, Arnett KL, Bayston LJ, Liao W, Proby CM, Leigh IM, Collisson EA, Gordon PB, Jakkula L, et al. Loss-of-function mutations in Notch receptors in cutaneous and lung squamous cell carcinoma. Proc Natl Acad Sci U S A. 2011; 108:17761–17766. [PubMed: 22006338]

Wendorff AA, Koch U, Wunderlich FT, Wirth S, Dubey C, Bruning JC, MacDonald HR, Radtke F. Hes1 is a critical but context-dependent mediator of canonical Notch signaling in lymphocyte development and transformation. Immunity. 2010; 33:671–684. [PubMed: 21093323]

Weng AP, Ferrando AA, Lee W, Morris JPt, Silverman LB, Sanchez-Irizarry C, Blacklow SC, Look AT, Aster JC. Activating mutations of NOTCH1 in human T cell acute lymphoblastic leukemia. Science. 2004; 306:269–271. [PubMed: 15472075]

Yashiro-Ohtani Y, Wang H, Zang C, Arnett KL, Bailis W, Ho Y, Knoechel B, Lanauze C, Louis L, Forsyth KS, et al. Long-range enhancer activity determines Myc sensitivity to Notch inhibitors in T cell leukemia. Proc Natl Acad Sci U S A. 2014; 111:E4946–4953. [PubMed: 25369933]

Yatim A, Benne C, Sobhian B, Laurent-Chabalier S, Deas O, Judde JG, Lelievre JD, Levy Y, Benkirane M. NOTCH1 nuclear interactome reveals key regulators of its transcriptional activity and oncogenic function. Mol Cell. 2012; 48:445–458. [PubMed: 23022380]

Zeytuni N, Zarivach R. Structural and functional discussion of the tetra-trico-peptide repeat, a protein interaction module. Structure. 2012; 20:397–405. [PubMed: 22404999]

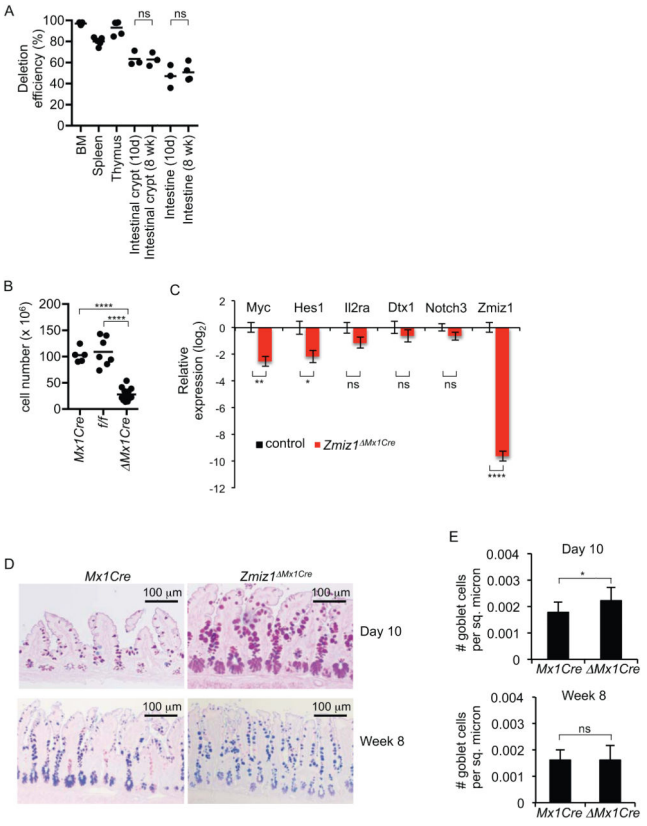

Figure 1. Deletion of *Zmiz1* inhibited T-cell development and transiently induced goblet cell hyperplasia

(A) QPCR showing *Zmiz1* deletion efficiency in BM (n=5 mice), spleen (n=5 mice), thymus (n=5 mice), and intestine (n=3 mice) at 8 weeks after end and 10 days after start of pIpC. (B) Thymus cellularity of *Mx1Cre* (n=5 mice), $Zmiz1^{f/f}$ (n=7 mice) and $Zmiz1^{\Delta Mx1Cre}$ (n=13 mice) mice at 8 weeks after end of pIpC treatment. One experiment was performed. (C) LOG_2 scale qPCR showing relative mean transcripts of five Notch1 target genes and Zmiz1 relative to 18S expression in sorted DN3 cells from paired control and $Zmiz1^{\Delta Mx1Cre}$ mice (n=4 mice except Notch3 and Zmiz1, n=3 mice). Data are mean + s.e.m. (D and E) Goblet cells were stained with Periodic Acid-Schiff/Alcian Blue in ileum sections at 10x magnification (D) and quantified per area (E) from *Mx1Cre* (n=3 mice, 12 villi per mouse) and $Zmiz1^{\Delta Mx1Cre}$ (n=3 mice, 12 villi per mouse) mice at 10 days after initiation or 8 weeks after end of pIpC. Two independent experiments were performed. *P<0.05; **P<0.01; ***P<0.001; ****P<0.0001. See also Figures S1 and S2.

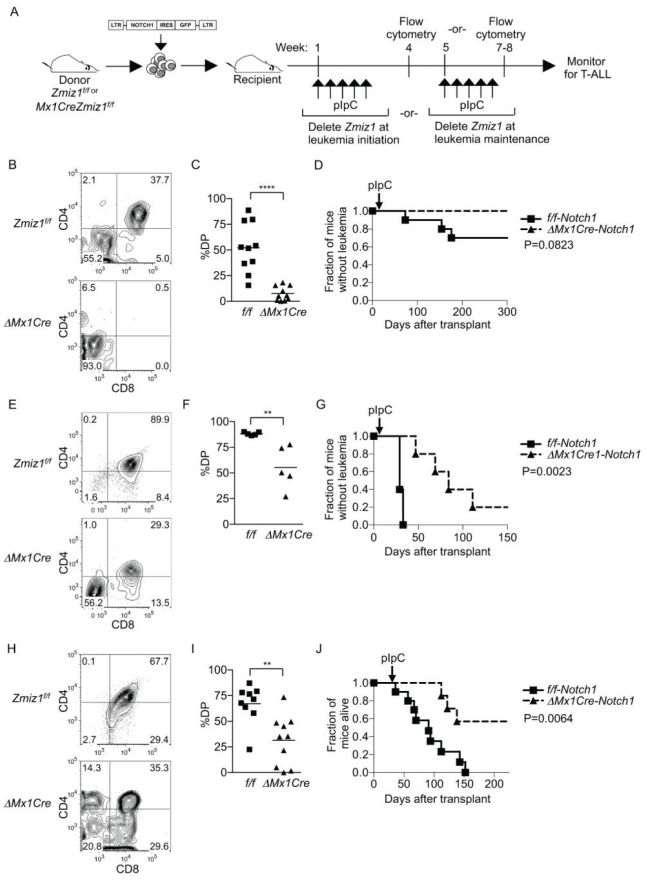

Figure 2. Zmiz1 is important for initiation and maintenance of T-cell leukemia

(A) Schematic of retrovirally induced BMT model of Notch-induced leukemia. (B–G) Flow cytometry T-cell plots of transduced blood cells at 4 weeks post-transplant (B and E), %double-positive (DP, $CD4^+CD8^+$) transduced blood cells at 4 weeks post-transplant (C and F), and fraction of mice with leukemia (D and G) transplanted with L1601PΔP (B–D) or ΔEGFΔLNRΔP (E–G) expressing *Zmiz1*$^{f/f}$ and *Mx1CreZmiz1*$^{f/f}$ progenitors (n=10 mice per group for B–D; 5 mice per group for E–G). PIpC was injected 1 week after transplant to delete *Zmiz1*. (H–J) Flow cytometry T-cell plots of transduced blood cells (H), %double-positive (DP, $CD4^+CD8^+$) transduced blood cells at 2–3 weeks after pIpC injection (I), and survival (J) of mice transplanted with ΔEGFΔLNRΔP-expressing *Zmiz1*$^{f/f}$ (n=10 mice) and *Mx1CreZmiz1*$^{f/f}$ (n=7 mice) progenitors. PIpC was injected ~5 weeks after transplant when WBC was detected above 100K/μl. One experiment was performed. **P<0.01; ****P<0.0001. See also Figure S3.

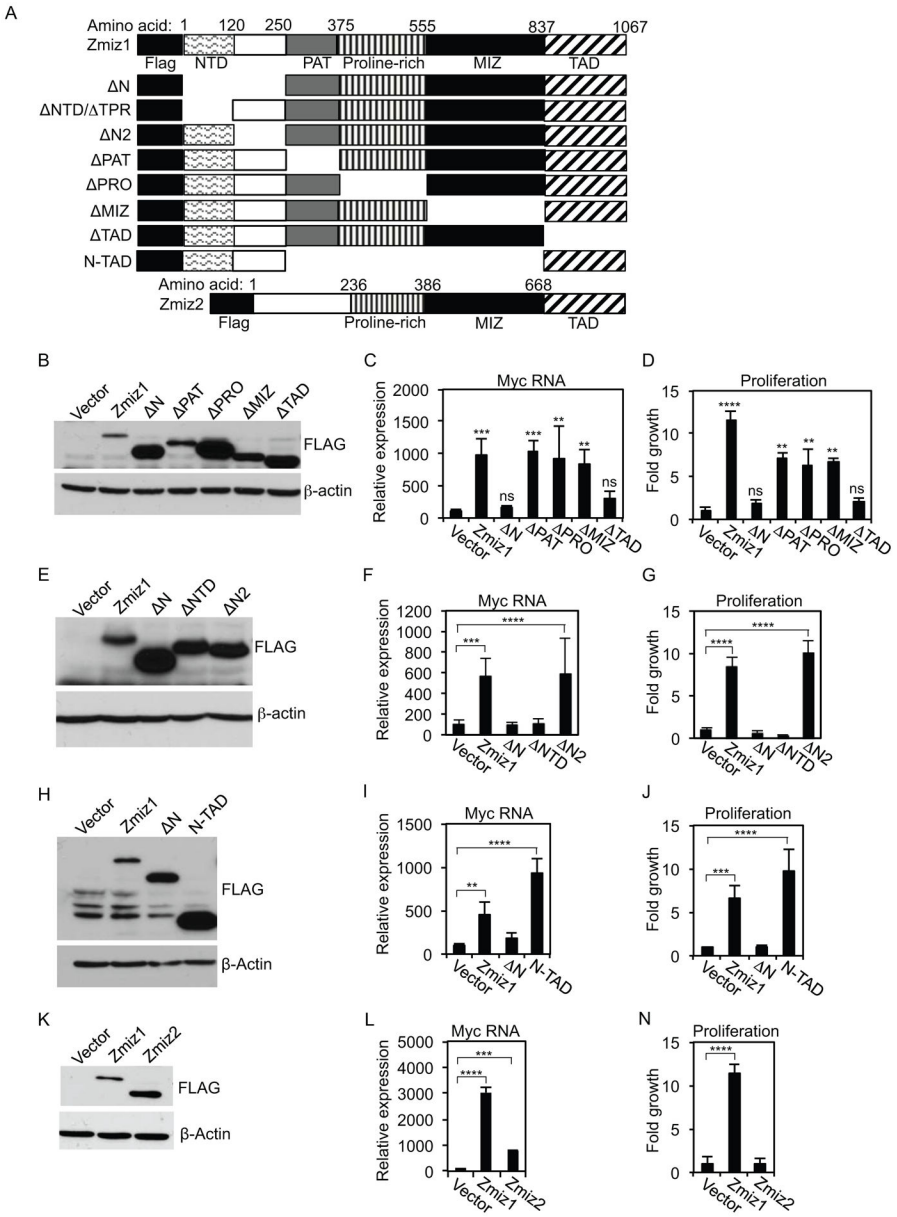

Figure 3. The N-terminal domain (NTD) of Zmiz1 is important for driving Myc transcription and proliferation

(A) Domain structure of Zmiz1, Zmiz2, and deletion mutants. (B–N) Western blot using the FLAG antibody showing that all tested proteins were expressed at levels equal to or greater than wildtype Zmiz1 (B, E, H, and K), qPCR analysis for Myc transcripts relative to the empty vector (C, F, I, and L), and fold increase in cell number relative to the empty vector after 6 days of culture (D, G, J, and N) of sorted 8946 cells that were transduced with the indicated Zmiz1 constructs and L1601PΔP. At least two independent experiments were performed. *P<0.05; **P<0.01; ***P<0.001; ****P<0.0001.

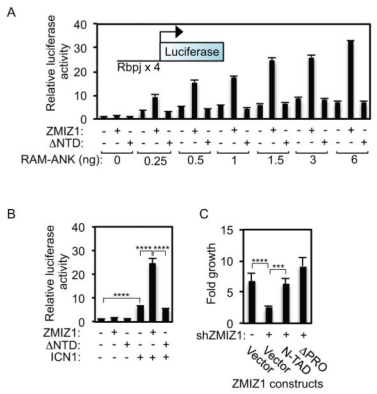

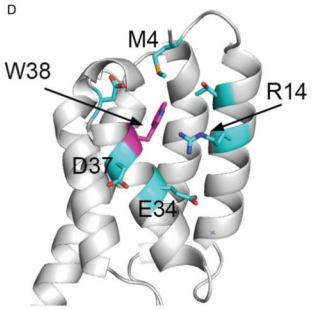

E

Transcription factors interacting with the TPR bait but not control		
Transcription factor	#unique peptides	#independent spectra
Notch1	38	171
Zmiz1(bait)	31	327
Maml1	13	24
Kap1/Trim28	11	21
Rbpj	11	22
Satb1	7	8
Nfatc3	7	12
Ctnnb1	6	8
Zeb1	6	9
Evi1	3	12
Brca1	3	4
Bclaf1	3	4
Tcf7	2	4
Sirt1	2	3

Figure 4. The N-terminal domain (NTD) of Zmiz1 is important for enhancing Notch reporter activity and contains tetratricopeptide repeats (TPR) that mediate protein-protein interactions

(A and B) Luciferase activity in U2OS cells transfected with 250 ng Notch-dependent (Rbpjx4) luciferase reporter, 100 ng Zmiz1 or ΔNTD, RAM-ANK (A) or 0.5 ng ICN1 (B). Data are relative to control cells. At least two independent experiments were performed. (C) Fold growth of human T-ALL cells (CEM/SS) co-transduced with shControl (−) or shZMIZ1_1 (+) and the ZMIZ1 mutants N-TAD or ΔPRO after 3 days of culture. Since shZMIZ1_1 recognizes the PRO domain it would not target N-TAD or ΔPRO. (D) Crystal structure of the NTD domain shows tandem tetratricopeptide repeats (TPR) with mapped interface involved in Notch1 binding. (E) Mass spectrometry results showing all known transcriptional regulators ranked by number of unique peptides (at least 2) that were immunoprecipitated by FLAG antibody in 8946 cells transduced with the FLAG-TPR bait but not with the empty vector control. One experiment was performed.

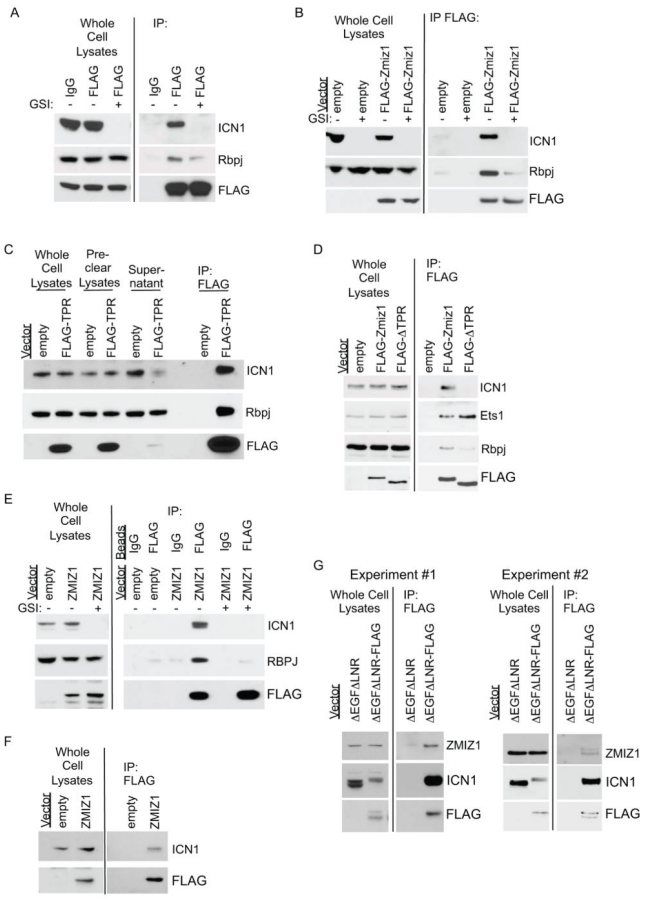

Figure 5. Zmiz1 interacts with Notch1

(A–D) Co-IP using the control IgG (A) or FLAG (A–D) antibody in 8946 cells co-transduced with L1601PΔP and the empty vector control (B–D), FLAG-Zmiz1 (A, B and D), FLAG-TPR (C), or FLAG-ΔTPR (D) to identify co-bound ICN1, endogenous Rbpj, and endogenous Ets1 (D) and the response to GSI (A and B). (E) Co-IP using the control IgG or FLAG antibody in THP6 cells transduced with empty vector or FLAG-ZMIZ1 to identify co-bound ICN1 and RBPJ in response to GSI. (F) Co-IP using the FLAG antibody in CEM/SS cells transduced with FLAG-ZMIZ1 to identify co-bound ICN1. (G) Two independent co-IP experiments using the FLAG antibody in CEM/SS cells transduced with ΔEGFΔLNR or ΔEGFΔLNR-FLAGx2-HAx2 (“ΔEGFΔLNR- FLAG”) to identify co-bound endogenous ZMIZ1. At least two independent experiments were performed.

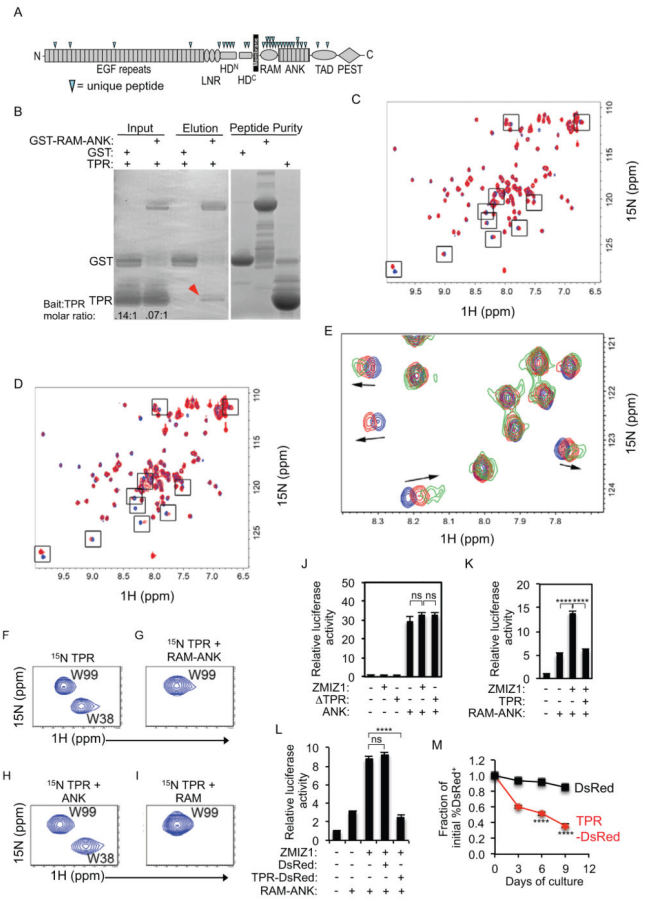

Figure 6. The TPR domain of Zmiz1 binds directly to the RAM domain of ICN1

(A) Schematic of Notch1 showing that the unique peptides identified by the MS screen were clustered around RAM-ANK. (B) GST pull-down assay stained with Coomassie blue using 30 μg GST or GST-RAM-ANK as bait for 120 μg TPR at indicated molar ratios. Red arrowhead identifies TPR pulled down by GST-RAM-ANK but not GST. (C and D) ^{1}H-^{15}N HSQC spectrum for 50 μM ^{15}N TPR (blue) and 50 μM (C) or 100 μM (D) unlabeled RAM-ANK (red). (E) Fragment of ^{1}H-^{15}N HSQC spectra for 50 μM ^{15}N TPR (blue) and with 50 μM RAM-ANK (red) or 100 μM RAM-ANK (green) showing chemical shift perturbations and peak broadening (arrows). (F–I) Small segments of ^{1}H-^{15}N HSQC spectra for ^{15}N TPR (F) and ^{15}N TPR mixed with RAM-ANK (G), ANK (H), or RAM (I). Direct binding causes loss of the W38 peak but not the W99 peak because W38 is very close to the binding interface. (J) Reporter activity in U2OS cells transiently transfected with a Notch-dependent (Rbpjx4) luciferase reporter (250 ng), Zmiz1 or ΔTPR (100 ng), and ANK (100 ng). (K and L) Luciferase reporter activity in U2OS cells transiently transfected with a Notch-dependent (Rbpjx4) reporter (250 ng), Zmiz1 (100 ng), RAM-ANK (6 ng), TPR (K, 100 ng), and TPR-DsRed fusion protein (L, 100 ng) to test TPR as a dominant negative Zmiz1 inhibitor. (M) 8946 cells transduced with L1601PΔP, Zmiz1, and TPR-DsRed were measured for fraction of %DsRed^{+} cells on Day 0 in doxycycline for 9 days. At least two independent experiments were performed. *P<0.05; ****P<0.0001.

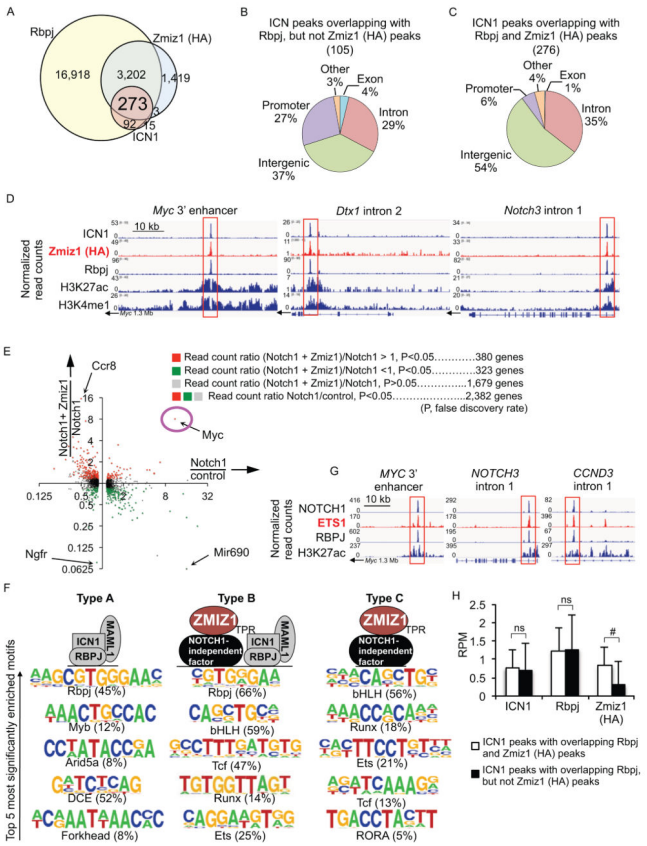

Figure 7. Zmiz1 selectively regulates a subset of Notch1 target genes and binds a unique class of Notch1-regulatory sites

(A) Intersection averages of Zmiz1, ICN1, and Rbpj sites identified by ChIP-Seq in 8946 cells transduced with HA-Zmiz1 and activated Notch1. (B and C) Intersection analysis showing ICN1 peaks co-bound with Rbpj and without Zmiz1 (B) or with Zmiz1 (C). (D) ICN1, Zmiz1 (HA), and Rbpj aligned normalized read counts and associated histone marks in the *Myc* 3′ enhancer, *Dtx1* intron 2, and *Notch3* intron 1. (E) RNA-Seq dot plot of 2,382 Notch target genes (see Figure S6A). The genes in each quadrant with the largest fold change upon further addition of Zmiz1 are indicated. (F) Homer motif analysis showing the top five most significantly enriched transcription factor motifs in rank order lying + 250 bp of ICN1/Rbpj binding sites not associated with Zmiz1 (HA) binding sites (Type A); lying + 250 bp of Zmiz1 (HA) binding sites associated with ICN1/Rbpj binding sites (Type B); and lying + 250 bp of Zmiz1 (HA) binding sites not associated with ICN1/Rbpj binding sites (Type C). Percent of sites with the indicated motif is shown in parentheses. (G) ICN1, ETS1, and RBPJ aligned normalized read counts from GSE51800(Wang et al., 2014). (H) RPMs are shown for ICN1 peaks with overlapping Rbpj, and Zmiz1 (HA) peaks (C) and with overlapping Rbpj, but not Zmiz1 (HA) peaks (B). #P=3.717E-16. One experiment was performed. DCE=Downstream core element. See also Figures S4–S7.